RESEARCH ARTICLE

WILEY

Evaluating a novel MR-compatible foot pedal device for unipedal and bipedal motion: Test–retest reliability of evoked brain activity

Jade D. Doolittle[1] ◉ | Ryan J. Downey[2,3] | Julia P. Imperatore[1] |
Logan T. Dowdle[4,5] | Daniel H. Lench[4] | John McLeod[1] | Daniel M. McCalley[4] |
Chris M. Gregory[2] | Colleen A. Hanlon[1,6] ◉

[1]Department of Psychiatry and Behavioral Sciences, Medical University of South Carolina, Charleston, South Carolina

[2]Department of Health Sciences and Research, Medical University of South Carolina, Charleston, South Carolina

[3]J. Crayton Pruitt Family Department of Biomedical Engineering, University of Florida, Gainesville, Florida

[4]Department of Neurology, Medical University of South Carolina, Charleston, South Carolina

[5]Center for Magnetic Resonance Research (CMRR), University of Minnesota, Minneapolis, Minnesota

[6]Department of Cancer Biology, Wake Forest University, Winston-Salem, North Carolina

Correspondence
Colleen A. Hanlon, Department of Psychiatry and Behavioral Sciences, Medical University of South Carolina, Institute of Psychiatry, 67 President St, MSC 861, Charleston, SC 29425.
Email: chanlon@wakehealth.edu

Funding information
National Center of Neuromodulation for Rehabilitation, Grant/Award Number: P2CHD0886844; National Institute of General Medical Sciences, Grant/Award Number: P20GM109040

Abstract

The purpose of this study was to develop and evaluate a new, open-source MR-compatible device capable of assessing unipedal and bipedal lower extremity movement with minimal head motion and high test–retest reliability. To evaluate the prototype, 20 healthy adults participated in two magnetic resonance imaging (MRI) visits, separated by 2–6 months, in which they performed a visually guided dorsiflexion/plantar flexion task with their left foot, right foot, and alternating feet. Dependent measures included: evoked blood oxygen level-dependent (BOLD) signal in the motor network, head movement associated with dorsiflexion/plantar flexion, the test–retest reliability of these measurements. Left and right unipedal movement led to a significant increase in BOLD signal compared to rest in the medial portion of the right and left primary motor cortex (respectively), and the ipsilateral cerebellum (FWE corrected, $p < .001$). Average head motion was 0.10 ± 0.02 mm. The test–retest reliability was high for the functional MRI data (intraclass correlation coefficients [ICCs]: >0.75) and the angular displacement of the ankle joint (ICC: 0.842). This bipedal device can robustly isolate activity in the motor network during alternating plantarflexion and dorsiflexion with minimal head movement, while providing high test–retest reliability. Ultimately, these data and open-source building instructions will provide a new, economical tool for investigators interested in evaluating brain function resulting from lower extremity movement.

KEYWORDS
bipedal movement, brain activity, fMRI, lower extremity, motor impairment, MR-compatible device, rehabilitation

1 | INTRODUCTION

Lower extremity function (e.g., dorsiflexion/plantarflexion) is often affected in individuals with movement disorders and impairments in these movement patterns contribute to high rates of morbidity and mortality in these patients (Wenning et al., 2005). For example, impaired dorsiflexion resulting in "foot-drop" and the resulting gait impairments following stroke and other neurological disorders (e.g., dystonia in Parkinson's disease, spasticity in multiple sclerosis, and spinal cord injury) increase the risk for falls, contribute to poor balance, and cause immobility that can lead to more severe health factors (da Cunha, et al., 2002). Similarly, plantar flexor dysfunction results in a reduction of propulsion during walking and explains 67–72% of the variance in walking function poststroke and is a primary impairment in many neurological injuries or diseases (Williams, Schache, & Morris, 2012). Consequently, physical rehabilitation strategies often focus on improving isolated dorsiflexion and plantar flexion with the hopes of enhancing reciprocal bipedal movement fluidity in these clinical cohorts (Xiao, Huang, & O'Young, 2012) (Dobkin & Dorsch, 2013). To date, rehabilitation efficacy has primarily relied on behavioral outcome measures including gait speed, efficiency, and muscle strength (Latham et al., 2005) or biomarkers for neurological recovery (Milot & Cramer, 2008). Given that it is often a neurologic insult that leads to resultant disability, optimizing rehabilitation strategies will require that investigators learn more about the function and/or adaptations in the neural circuitry that underline movement dysfunction in these patients. To date however, this has not been well studied, due in part, to a lack of robust magnetic resonance imaging (MRI)-compatible foot pedal devices that are readily available to the clinical research community for reliably assessing lower extremity function.

From a neural perspective, gait is an inherently rhythmic, coordinated, bilateral process which requires the brain to shift activity from the left to right motor networks and back again. Previous work has shown that actual bipedal movement causes greater neural activity than mental imagery of bipedal movement (Labriffe et al., 2017). Recently, it has also been shown to stimulate greater neural activity than unipedal movement (Noble, Eng, & Boyd, 2014). However, to date, technical limitations of functional MRI (fMRI) has limited the evaluation of lower extremity motor performance to unilateral tasks involving single-joint(Sahyoun, Floyer-Lea, Johansen-Berg, & Matthews, 2004), unidirectional movements (e.g., isolated ankle dorsiflexion) (Trinastic et al., 2010) (Ciccarelli et al., 2005; Grooms et al., 2019; Newton et al., 2008) bicycling movements (which are often associated with a lot of head movement) (Fontes et al., 2015; Mehta, Verber, Wieser, Schmit, & Schindler-Ivens, 2009; Promjunyakul, Schmit, & Schindler-Ivens, 2015), or balance control movements (Karim et al., 2014). Concomitant head movement while performing these lower extremity tasks has impaired researchers' ability to clearly identify the brain dynamics associated with alternating bipedal movement (Papegaaij et al., 2017).

The goal of this study was to develop an open-source bipedal device that could be used in the MRI scanner to robustly evaluate neural networks involved in rhythmic dorsiflexion and plantarflexion with one or both feet. Although several foot pedal devices have been developed for the MR-environment, many of these devices are unipedal and not capable of being used to evaluate the rhythmic movement associated with bilateral movement (Newton et al., 2008; Promjunyakul et al., 2015; Trinastic et al., 2010). Furthermore, previous studies investigating the use of MRI compatible devices have not reported angle metrics of joint function (e.g., angles, torques, etc.) and have been performed in relatively small participant samples (Newton et al., 2008). Recently there has been a greater interest in the neural networks associated with bipedal movement, and correspondingly several groups have been developing unique devices (Belforte & Eula, 2012; de Lima-Pardini et al., 2017; Hollnagel et al., 2011; Ikeda et al., 2015; Jaeger et al., 2014; Martinez et al., 2014; Noble et al., 2014). Jaeger et al. (2014) developed an elegant stepping device for the MRI scanner and demonstrated robust neural activity associated with bilateral stepping. These devices however are not widely available for use by investigators interested in studying underlying brain mechanisms associated with gait-like movements. Here we aimed to develop a simplified pedal device that could accurately quantify ankle joint movement while also extracting information regarding the brain networks involved in bipedal movement. By accessibility to a device with high test–retest reliability, clinicians may be better equipped to measure rehabilitative interventions in clinical populations.

Following iterative device development, we collected test–retest reliability data in a cohort of healthy controls performing alternating unilateral and bilateral plantarflexion and dorsiflexion at a rate and resistance that would be applicable to future clinical studies of locomotor function. We ultimately would like to use this device as a feasible measurement tool of current rehabilitation interventions and their success while also providing a resource for measuring blood oxygen level-dependent (BOLD) signal changes during lower extremity tasks to combat the issue of technical limitations such as head motion.

2 | METHODS

2.1 | Subjects

Twenty healthy controls (12 males and 8 females, average age 26 years old, range 21–37) with no history of neurological injury or disease, or a history of musculoskeletal pathology were recruited from the local community with digital advertisements and word-of-mouth advertising. Each participant signed a consent approved by the Institutional Review Board of the Medical University of South Carolina. After the opportunity to ask questions, the Edinburgh Handedness Inventory was administered to determine dominant handedness as handedness and foot preference are related in most individuals (Barut, Ozer, Sevİnc, Gumus, & Yunten, 2007). In addition, standard MRI safety screening was performed for each participant. Participant's feet were then calibrated to the device and strapped into place across the dorsum (top of the foot) to ensure secure placement. A lower extremity alternating bipedal dorsiflexion/plantarflexion task (described below) was completed within the 3 T Siemens PRISMA MRI scanner.

The study consisted of two fMRI visits separated by approximately 2–6 months—which is consistent with longitudinal assessment time points of clinical trials with individuals undergoing gait rehabilitation training.

2.2 | Device design and assembly

The final prototype of the bipedal device (Figure 1) was designed after iterative pilot testing for safety and participant comfort (see Supplemental Data for parts list and assembly instructions). The apparatus was composed of a mixture of aluminum (78% by weight); various types of stainless steel (14% total weight: 6% 18–8, 2% 304, 1% 316, 5% unspecified); plastic (6%); rubber (1%); glass/ceramic (<1%); and fluid (<1%) and weighed approximately 15.4 kg. Although the vast majority of the device was nonferrous by weight, we could not completely eliminate the use of stainless steel. Thus, once the first prototype was built, the device was deconstructed into sub-assemblies, and we iteratively introduced the device to the static magnetic field of the scanner, including a greater percentage of the stainless-steel parts with each iteration to ensure safety in the MR environment.

The frame of the device was constructed out of T-slotted aluminum bars (80/20 Inc.), fastened with stainless steel screws and nuts (80/20 Inc.; McMaster-Carr). The use of T-slotted bars provided us with the flexibility to easily fine tune the geometry of the device during development. Along these lines, the device accommodates for anatomical differences between individuals and physical differences in footwear so that each subject's ankle joint can be aligned with the axis of rotation of the device. A hook and loop strap secured each person's feet to the device.

Aluminum reaction torque sensors (Transducer Techniques, TRS-2K) were placed in line with the axis of rotation of the device. Each torque sensor was attached to a foot pedal on one end and a custom 3D printed pulley on the opposite end. A stretchable elastic band (TheraBand, silver resistance tubing) was attached to the pulley to assist in lifting the foot into a resting position (i.e., relieve the gravitational pull of the foot pedal on the subject) and to provide a resistive torque to plantar flexion. The tension of the elastic band is adjustable via a plastic ladder strap (M2 Inc., LS75) and an aluminum ratcheting mechanism (M2 Inc., RB75-ALU-T). An inclinometer (Spectron, Spectrotilt SSY0185-VHR) was attached to the outside of the pulley to measure the angle of the pedal with respect to ground (Figure 1). The inclinometer is a glass/ceramic hybrid electrolytic sensor suspended in fluid and housed in aluminum where the fluid viscosity was customized for our specific application to allow us to measure faster angular velocities.

The torque sensor signals are amplified by signal conditioners (Transducer Techniques, TMO-2) placed outside the scanner while torque and angle signals are recorded by a data acquisition device (Quanser, Q8-USB) via Simulink (MathWorks). Similarly, a trigger signal (0–5 V square pulse train) was routed from the scanner to the data acquisition device so that angle and torque data could be synchronized to each volume capture.

2.3 | Study procedures

Prior to beginning MRI procedures, the bipedal device was calibrated for each individual outside the scanner based on foot size and structure, such that the ankle joint was aligned with the axis of rotation of the device for reliable angular kinematic measurements. The bipedal device was then placed on the end of the bed of the MRI scanner, and the participant's feet were secured with the hook and loop straps. To prevent significant head movement as a result of completing the task, the device was positioned for each subject such that their knees were slightly bent (10–15° of flexion), with cushions placed below the knees for support.

A high-resolution MEMPRAGE anatomical image was collected (voxel size: 1 mm^3; TR/TI 2,530/1,200 ms; TEs: 1.69, 3.55, 5.41, 7.27 ms; FA: 7°; TA: 7:00). Two identical sessions of whole-brain, BOLD-weighted data were collected using a multiband sequence (Multiband 3, TR: 1,000 ms; TE: 30 ms; FA: 50°; TA 5:24). In addition, we collected a fieldmap image with matching voxel dimensions and brain coverage to correct for image distortion. The residual mean
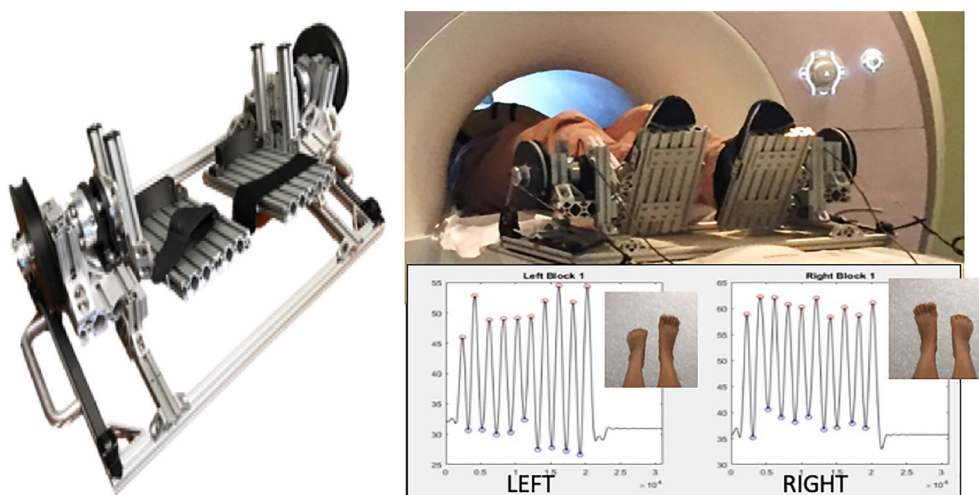

FIGURE 1 MR-compatible bipedal gait device and quantitative measure of angle output during left versus right foot movement blocks

squared output from the MEMPRAGE was used for subsequent analysis steps.

Participants returned for a follow-up visit approximately 2–6 months following Visit 1. All procedures were identical to the first visit.

2.4 | Functional MRI unilateral and bilateral foot pedal task

An alternating bilateral and unilateral dorsiflexion-plantarflexion task was created using Eprime 3.0 software (Psychology Software Tools, Pittsburgh, PA). The task consisted of eight task blocks (right only, left only, both, and rest) which were presented in a randomized order. During the movement blocks (20 s) participants were asked to mimic a video of rhythmic dorsiflexion (2 s) and plantarflexion (2 s) movements. During the rest block (20 s), the participants viewed an image of feet that remained in a stable position. There were also "preparation" events (3 s) during which participants were instructed to prepare for motion.

Each participant attended two study visits. Each study visit consisted of anatomical images as well as two sessions of the task. During each session, real-time feedback of the displacement was provided to researchers using digital information streaming from the pedal to the control room via a cord through the waveguide (as is standard with most MR research instruments). Prior to beginning the task, there was a practice session within the MRI scanner in which participants were instructed to closely mimic plantarflexion and dorsiflexion movements that were displayed on a projector screen.

Data were converted from DICOM format to NIfTI using dcm2niix. Anatomical images were processed with SPM12's Segment tool to calculate nonlinear deformations to MNI space. Functional data were processed in SPM12 using conventional processing steps including motion and distortion correction using a fieldmap. Functional data were coregistered to a skull stripped anatomical image and normalized to MNI space. Finally, the data were smoothed using a 6 mm FWHM Gaussian kernel.

For each individual, data from both Visits 1 and 2 were included into a general linear model of BOLD signal change. Each block (right only, left only, both, and rest) was modeled as a boxcar (task: 20 s, prepare screen: 3 s) convolved with the canonical hemodynamic response provided in SPM. Parameter estimates were generated at the subject level using the FAST option, in order to properly adjust for time series autocorrelation (Olszowy, Aston, Rua, & Williams, 2019). Primary contrasts of interest included: right foot versus rest, left foot versus rest, alternating both feet versus rest, and right versus left. The six motion parameters estimated during motion correction were also included in the model to account for variance in the BOLD signal due to head motion. The first-level SPM design matrix is provided in Supplemental Figure S2.

For the group, a one-sample t test of the contrast maps from the first-level within subject analysis described above was used to evaluate the consistency of brain engagement during each foot movement block. To evaluate test–retest reliability a secondary group analysis was done using a paired t test. A voxel level threshold of $p < .001$, uncorrected, and a cluster level threshold of $p < .05$ was used to identify regions of significant activation for the comparisons.

To further determine the reliability of the task, we calculated voxel-wise intraclass correlation coefficients (ICCs) using AFNI's 3dLME (Chen et al., 2018) using the estimated parameter maps, entered into separate models, with subject and visit corresponding to random effects. ICC maps were interpreted using conventional approaches, with 0–0.4 corresponding to "poor," 0.4–0.6 to "fair," 0.6–0.75 as good and greater than 0.75 as excellent reliability (Cicchetti, 1994).

2.5 | Quantitative motion measures

The bipedal device was designed to allow unipedal and bipedal motion that is limited to the lower extremities such that the quality of the fMRI data is not affected by excessive head movement. We examined the average motion that occurred during each session, as well as the average motion occurring specifically during each of the blocks (right only, left only, both, and rest) within sessions.

Angle sensors incorporated in the device collected quantitative range of motion data. Minimum and maximum peaks for each movement type were extracted from the angle recordings using custom MATLAB scripts (MATLAB, MathWorks (2017a)). These data from both visits were then compared in order to determine if there was any significant difference in overall displacement between visits. The data was then used to evaluate overall reliability using ICCs.

Average displacement was calculated for each movement and rest block. During bipedal movement, left and right feet were averaged to gather displacement across limbs. All statistical data were analyzed using the SPSS statistical program (SPSS, IBM Statistics for Macintosh version 25.0).

3 | RESULTS

3.1 | Motion parameter reliability analyses

The mean, SD and range of angular displacement are displayed in Table 1, with the data from each participant's Visits 1 and 2 listed separately. Overall, there was very high test–retest reliability. ICC for angular displacement was 0.842, suggesting excellent reliability of overall foot motion. Both ICC values for moving the right foot only (0.825, $F(10,10) = 5.720$, $p = .005$)) and for moving left foot only (0.819, $F(10,10) = 5.543$, $p = .006$) support excellent reliability of unipedal motion. In addition, during bipedal motion, both the right and left feet (0.878, $F(10,10) = 8.176$, $p = .001$) have high reliability, providing evidence that bipedal motion with this device is reproducible over time scales historically used in clinical trials for gait disorders. Angle displacement across visits was calculated (Visits 1 and 2) and plotted for each of the subjects (Figure 2).

TABLE 1 Table with descriptive statistics of angle data (in degrees) between sessions and across visits

	Visit 1, Session 1			Visit 1, Session 2			Visit 2, Session 1			Visit 2, Session 2		
	Left	Right	Both	Left	Right	Both	Left	Right	Both	Left	Right	Both
Range	36.98°	36.95°	35.11°	28.26°	24.90°	27.54°	33.13°	40.30°	35.50°	42.70°	40.60°	37.46°
Mean	36.54°	35.09°	34.11°	36.29°	35.41°	35.79°	34.75°	33.88°	34.01°	35.24°	33.76°	33.69°
SD	10.91°	10.78°	10.37°	8.09°	7.85°	8.51°	7.90°	9.52°	8.98°	9.80°	9.83°	9.62°

Note: N = number or subjects, range = range of displacement across subjects, mean = mean displacement of overall movement for each block, SD = standard deviation of overall movement for each block.
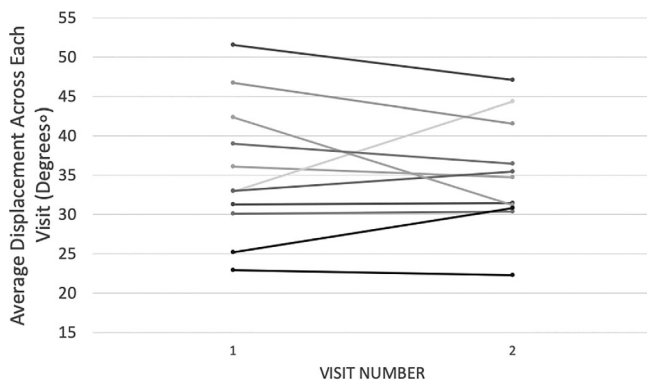
FIGURE 2 Angle displacement from output of the bipedal device across visits was calculated (Visits 1 and 2) and plotted for each of the subjects

3.2 | Head motion estimates

The average motion throughout each session and across visits was very low: 0.10 ± 0.02 mm. Examining only the motion during each of the tasks, average movement was 0.097 ± 0.028 mm across subjects. An overview of motion is provided in Supplemental Figure S1, which shows motion averaged across subjects, visits, and sessions for each of the six parameters, as well as the overall motion displacement.

3.3 | Task-related BOLD signal during left and right foot movement

Ankle range of motion was associated with strong activation in consistent areas of the lower limb motor network across each motion during the Gait–Mate task and across visits. For Visit 1, right foot motion resulted in significant activation (voxel $p < .001$, $p_{FWE} < .05$) in the left motor cortex, premotor cortex, secondary somatosensory cortex, putamen, visual cortex, and the right cerebellum (Figure 3, Table 2). For left foot motion, significant activation (voxel $p < .001$, $p_{FWE} < .05$) was found in the right motor cortex, premotor cortex, secondary somatosensory cortex, putamen, and the left cerebellum. For bilateral movement, significant activation (voxel $p < .001$, $p_{FWE} < .05$) was found in the left and right motor cortex, premotor cortices, secondary somatosensory cortices, putamen, and the right and left cerebellum. Left foot movement showed significantly more activation in the right

motor cortex, premotor cortex, and left thalamus, and secondary somatosensory region than right foot movement. Results from the second visit, occurring 2–6 months later, were similar (quantified below) to visit 1. Paired t tests did not show differences in activation between Visits 1 and 2. BOLD signals were compared between left hand dominant $n = 10$, score = −70 and right hand dominant individuals $n = 10$, score = 86 (score > (+40) = right-handed, score < (−40) = left-handed, and any score in between = ambidextrous) and found no significant difference in activation.

3.4 | Reliability analyses

A comparison of Visit 1 versus Visit 2 for each individual yielded high ICC values throughout much of the brain—including the primary motor cortex and somatosensory regions having strong ICC values (>0.75, Figure 4). The mean ICC values across all gray matter were 0.36 ± 0.21, 0.38 ± 0.21, and 0.38 ± 0.21 for right, left, and both feet, respectively.

4 | DISCUSSION

The development of novel, targeted interventions for neurological diseases that affect walking would be significantly advanced by the ability to evaluate the underlying neural basis of lower extremity dysfunction and impairment as well as recovery following treatment. In this study, we describe an MR-compatible device which allows for the simultaneous measurement of brain activity and biomechanical features of lower-limb movement (in particular bipedal ankle movement). Our device allows for little head movement during lower extremity engagement and could be used to assess motor dysfunction in different clinical populations in the future. Our device produced reliable brain activation within-individuals across therapeutic timescales (approximately 2–6 months) and was not associated with excessive amounts of head motion (with mean movement of approximately 0.1 mm). Quantitative angle displacement metrics were collected using the MR-compatible device to ensure quality control and task performance consistency across visits. These metrics were shown to produce reliable results as well. Overall, we demonstrate this innovative MR-compatible device which can be used as an effective tool to evaluate cortical activation during lower extremity bipedal motion.
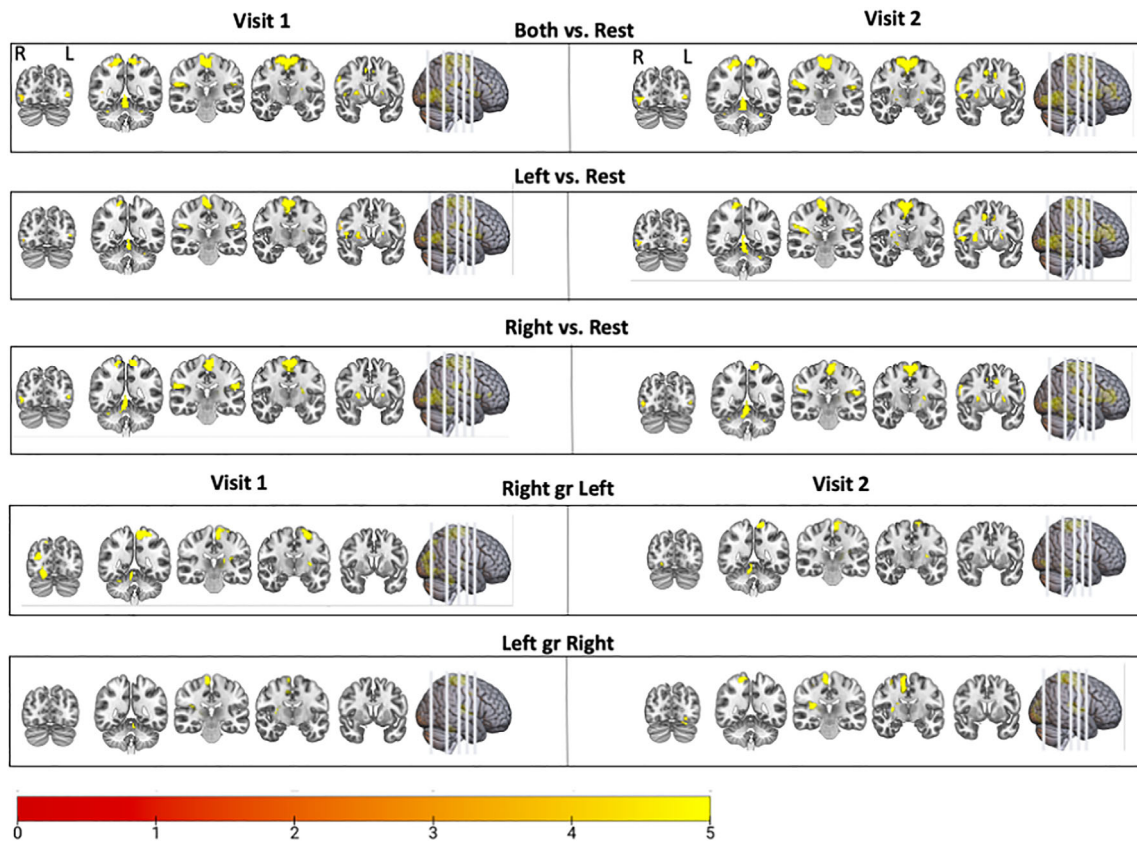
FIGURE 3 Blood oxygen level dependent (BOLD) signal during unipedal and bipedal movement. Participants were instructed to follow a video of foot dorsiflexion and plantarflexion movement. The task divided into blocks of left foot, right foot, left and right alternating (bipedal), and rest. The areas that were significantly activated following the movement blocks versus the rest blocks are shown (FWE corrected, $p < .05$) and described in more detail in Table 1. This is displayed for Visits 1 and 2. There was high test–retest reliability in activation

Unipedal and bipedal motion were associated with significant activity within the expected regions of the motor network including cortical and cerebellar regions. In addition, significant lateralized activation was found in subcortical areas, including the putamen, globus pallidus, and thalamus. Consistent with visual-motor tasks other cortical areas active during the task included the occipital cortex and primary and secondary somatosensory regions. In the present study, there was no significant difference in the BOLD signal between unipedal and bipedal motion in the regions of interest explored. In addition, there was no significant difference in the BOLD signal based on dominant handedness of participants. The ability to accurately quantify activation patterns is of significant interest when studying clinical cohorts as activation can change as a result of the injury or disease as well as following rehabilitation intervention. One important consideration in interpreting these findings of this study is that the rate of individual foot movement in the bipedal condition is approximately half that of motion in the unipedal motion because of the synchrony of bipedal movement. Additional motor literature has shown evidence to support that higher speeds of muscle movement (Jaeger et al., 2014) are associated with larger BOLD responses. Nevertheless, global brain activation remains larger, as both hemispheres are involved in task performance. Future work should attempt to disentangle the relationship between the rate of foot motion as it interacts with unipedal and bipedal activity.

Usage of the device was associated with little head movements in the present sample, with an overall average of 0.1 ± 0.02 mm and an average of 0.1 ± 0.03 mm during movement blocks. Head motion during movement blocks was significantly higher than motion during the rest blocks (all $p < <.001$); however, the magnitude of the effect is only 0.02 mm, which is 0.8% of a voxel. In the current sample, no subjects were excluded due to motion. In comparing these displacement values, as well as motion in each direction (Figure S1), we find that motion in this sample is lower than what is seen with pedaling-type devices, in which average motion exceeded 1 mm (Promjunyakul et al., 2015) or 0.41 mm (Mehta et al., 2009). Although we collected data through a bidirectional movement paradigm, our motion estimates are nearly equivalent (0.1 ± 0.02 vs. 0.09 ± 0.03 mm) to those found in studies focusing on unidirection motion (Grooms et al., 2019). Collectively, these results support that the use of the device in order to evaluate lower extremity performance, despite the requirement of lower extremity movement, is feasible in the MR environment. The ability to perform motor tasks with limited head movement was seen as the major technical hurdle to overcome in this study and future work involving patients with neurological injury or disease are thus warranted. The findings of low motion in this sample are encouraging, and suggest it will be feasible to collect relatively low motion data from patient populations.

TABLE 2 Areas of elevated BOLD response to movement tasks in the scanner relative to rest

	kE	Puncorr	Region	T_{max}	Z_{max}	MNI coordinates X	Y	Z
Visit 1								
Right vs. rest	459	p < .001	Right cerebellum (exterior), cerebellar vermal Lobules I–V	19.14	7.49	12	−43	−25
	1,347	p < .001	Left precentral gyrus, supplementary motor area	15.96	7.05	−3	−34	65
	500	p < .001	Right inferior occipital gyrus	10.3	5.92	45	−67	2
	602	p < .001	Middle occipital gyrus	9.08	5.58	−48	−28	20
	265	p < .001	Right parietal operculum (S2)	8.14	5.28	48	−25	23
	155	p < .001	Left inferior occipital gyrus	6.46	4.64	−48	−70	5
	195	p < .001	Right putamen	6.41	4.62	24	11	5
	54	p = .046	Left inferior occipital gyrus	5.83	4.36	−33	−91	−7
Left vs. rest	1,023	p < .001	Right precentral/postcentral gyrus (medial segment)	13.49	6.62	9	−40	74
	363	p < .001	Left cerebellum	12.14	6.35	−21	−34	−25
	369	p < .001	Right inferior occipital gyrus	10.8	6.04	45	−67	2
	298	p < .001	Right parietal operculum (S2)	8.78	5.49	48	−25	23
	438	p < .001	Right central operculum	7.88	5.19	48	2	2
	105	p < .001	Left central operculum/left precentral gyrus	7.86	5.18	−45	−1	8
	181	p < .001	Left parietal operculum (S2)	6.99	4.86	−45	−28	23
	138	p < .001	Left inferior occipital gyrus	6.41	4.62	−48	−70	5
	54	p = .005	Left superior parietal lobule	5.64	4.27	33	−37	47
	122	p < .001	Left putamen	5.63	4.26	−27	−4	14
Both vs. rest	569	p < .001	Right cerebellum (exterior)	14.64	6.83	12	−40	−25
	2,430	p < .001	Left/right precentral gyrus (medial segment), supplementary motor area	13.49	6.62	−3	−31	65
	822	p < .001	Right inferior occipital gyrus, S2	11.37	6.18	42	−67	2
	117	p < .001	Left parietal operculum (S2)/postcentral gyrus	6.93	4.84	−48	−28	20
	253	p < .001	Left inferior occipital gyrus	6.82	4.79	−48	−70	5
	96	p = .001	Left putamen	6.54	4.68	−27	−4	11
Left vs. right	343	p < .001	Right precentral gyrus (medial segment)	13.19	6.57	6	−22	65
	198	p < .001	Left cerebellum	12.7	6.47	−12	−40	−25
	287	p < .001	Right parietal operculum (S2), thalamus	9.99	5.84	30	−19	14
	51	p = .002	Right middle cingulate gyrus/supplementary motor area	5.85	4.37	6	−7	44
Right vs. left	996	p < .001	Right cerebellum, occipital fusiform gyrus	27.76	Inf	12	−43	−25
	1,124	p < .001	Left precentral gyrus (medial segment)	18.59	7.42	−6	−34	65
	260	p < .001	Left posterior insula, putamen, thalamus	8.52	5.41	−30	−19	14
	89	p < .001	Right superior parietal lobule	7.27	4.97	15	−76	50
Visit 2								
Right vs. rest	677	p < .001	Right cerebellum (exterior), vermis	20.09	7.6	12	−43	−25
	2,278	p < .001	Left precentral gyrus (medial segment)	11.53	6.22	−6	−31	65
	427	p < .001	Right inferior occipital gyrus	11.1	6.12	45	−67	2
	716	p < .001	Right middle frontal gyrus	8.28	5.33	24	44	11
	258	p < .001	Right parietal operculum (S2)/postcentral gyrus	7.46	5.04	42	−31	23
	63	p = .002	Right precentral gyrus	6.82	4.79	57	8	32
	168	p < .001	Middle temporal gyrus, inferior occipital gyrus	5.91	4.4	−42	−64	8
	54	p = .003	Right postcentral gyrus	5.27	4.09	12	−40	65

TABLE 2 (Continued)

	kE	Puncorr	Region	T_{max}	Z_{max}	MNI coordinates		
						X	Y	Z
Left vs. rest	563	p < .001	Left cerebellum (exterior), vermis	22.9	Inf	−18	−37	−25
	1,396	p < .001	Right precentral/postcentral gyrus (medial)/supplementary motor area	13.64	6.65	9	−37	74
	589	p < .001	Right inferior occipital gyrus	11.08	6.11	45	−67	2
	2,474	p < .001	Right posterior insula, S2, thalamus	10.4	5.94	30	−19	14
	195	p < .001	Left parietal operculum/postcentral gyrus	7.35	5	−48	−28	20
	363	p < .001	Left inferior occipital gyrus, middle temporal gyrus	6.21	4.53	−39	−73	5
	69	p = .001	Right cerebellum (exterior), brainstem	5.84	4.37	30	−40	−34
Both vs. rest	794	p < .001	Cerebellar vermis, left and right cerebellum (exterior)	18.01	7.34	0	−49	−10
	582	p < .001	Right inferior occipital gyrus	12.47	6.42	45	−67	2
	2,201	p < .001	Left precentral gyrus (medial segment)/left and right supplementary motor area/right postcentral gyrus (medial segment)	12.39	6.4	9	−40	74
	1,445	p < .001	Right parietal operculum (S2), posterior insula	9.31	5.65	48	−25	26
	593	p < .001	Left putamen, pallidum	7.3	4.98	−24	−1	14
	125	p < .001	Left central operculum/precentral gyrus	7.21	4.95	−45	2	5
	217	p < .001	Left parietal operculum/postcentral gyrus	7.09	4.9	−48	−28	20
	200	p < .001	Left inferior occipital gyrus	6.24	4.55	−42	−76	5
	89	p < .001	Right precentral gyrus	5.36	4.13	33	−7	53
	88	p = .001	Left inferior occipital gyrus	5.04	3.97	−24	−82	−1
Left vs. right	300	p < .001	Left cerebellum (exterior)	22.94	Inf	−18	−37	−25
	980	p < .001	Right precentral/postcentral gyrus (medial segment)	15.92	7.04	6	−22	65
	468	p < .001	Right posterior insula, putamen, thalamus	12.24	6.37	33	−22	14
	419	p < .001	Left occipital fusiform gyrus	7.96	5.22	−15	−91	−10
Right vs. left	320	p < .001	Right cerebellum (exterior), vermis	21.53	7.75	12	−40	−22
	624	p < .001	Left postcentral/precentral gyrus	13.35	6.6	−6	−34	65
	206	p < .001	Left thalamus	9.54	5.71	−18	−22	2
	108	p < .001	Right occipital fusiform gyrus	7.38	5.01	18	−85	−7

Note: N = 20; voxel threshold p < .001, uncorrected. Regions are significant at cluster-level p < .05, FWE corrected. Coordinates of peak activity reported.

The ability of the device to record range of motion data allowed for not only brain activity reliability testing, but also quantitative measures that record successful completion of the Gait–Mate task. Across visits, participants were able to reliably perform the task with the given instructions while significantly keeping consistent foot motion (all ICC's p < < .01). The reliable performance of the task is important to show in neurologically healthy individuals. Moving forward, the ability to accurately track and monitor an individual's range of motion during task performance could allow for the device to be used as a measurement tool for rehabilitation intervention studies. Each participant's angle trace can be modeled to determine if foot movement was occurring as instructed and compared across visits, demonstrating the reliability of the device paired with the instructed e-prime task.

Testing of the device was associated with highly reliable brain activation and quantitative measures. The visits were delayed with a minimum of approximately 2 months in order to mimic study designs that evaluate changes associated with therapeutic interventions, which historically occur over larger timescales. In this sample of healthy controls, there is little to no reason to believe that task performance would change after a delay of 2 months. With these findings, future work should use similar techniques to determine if a given therapy alters the BOLD response or if baseline brain responses are associated with certain clinical or functional outcomes.

Evaluating the device within the MR environment, we found no change in reference amplitude when our device was present. Regarding safety of the device, very few building parts are of concern as many are made of nonmagnetic material. However, it is important to note that building the device out of plastic or polymer materials could maximize the safety of the device and minimize any RF heating. While in the present study, we did not have any observable heating of the device, necessary insulation and grounding is necessary to ensure safe use of the device. In addition, since the device is in direct contact with the participants feet, the device should not be operated with bare feet.
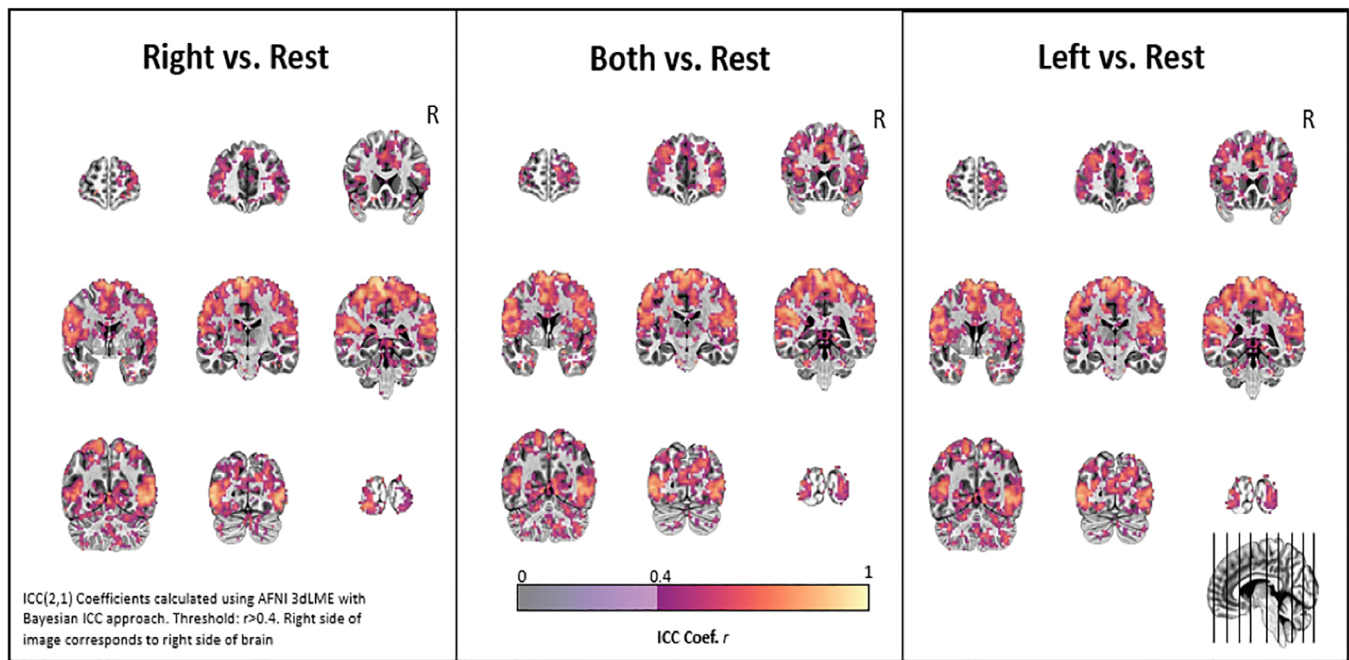
FIGURE 4 Test–retest reliability. The voxel-based interclass correlation coefficients on an individual subject basis are shown for movement with each pedal and both pedals versus rest for Visits 1 and 2. The coefficients were calculated with a Bayesian approach ($r > .4$, AFNI 3dLME)

There are a few limitations to this device and study. Notably, unlike more sophisticated bilateral stepping devices (Jaeger et al., 2014), the knees and hips remain in a relatively fixed position, which limits its applicability to real-world walking. That said, foot-drop and reduced propulsion contribute to a high degree of morbidity and mortality among stroke survivors with hemiplegia (Kluding et al., 2013), so assessing the impact of treatment on ankle function is still of great interest. Additionally, relatively simple low-cost design with open-access assembly instructions may prove to be a very scalable solution to clinical researchers across the globe. Another limitation is that contractile strength during the dorsiflexion/plantarflexion was not monitored in real time nor standardized between subjects. That said, the test–retest reliability within each person was very high from a neural activity perspective. Future studies will be necessary in order to determine if strength (or speed) of contraction and BOLD signal with this device are closely correlated. Furthermore, it would be useful for investigators to employ an assessment of foot dominance (e.g., Waterloo Assessment) rather than the EHI. Prospective longitudinal studies may want to consider addressing this limitation in order to more accurately standardize bipedal movements in populations with motor disorders. In addition, it is important to note that this study was completed in a healthy population and no participants were excluded from analysis due to excessive movement. While we found no significant head movement with the use of our device, future research should reassess this in a clinical population with movement disorders. Patients with lower extremity tremor in Parkinson's disease or muscle weakness causing more effortful task completion may pose a limitation with the device and add to overall movement artifact while in the scanner. On a broader scale, head movement during lower extremity engagement has been shown to be larger in older adults when compared to younger adults (Papegaaij et al., 2017). This is an important consideration when assessing individuals with movement disorders, who, on average, fall into this category.

5 | CONCLUSIONS

In this study, we present a rigorous set of feasibility and reliability data for a bipedal device which is capable of capturing BOLD signal fMRI data during lower extremity bipedal movement without significant head motion. We hope that by providing a parts list and open access instructions for assembly, other investigators will try to replicate these data at their own sites and further advance the knowledge of neuroplastic changes that occur during rehabilitation and therapeutic interventions. Brain activation data and quantitative measures make it a potentially useful device to be used in many clinical cohorts with movement disorders including, but not limited to, stroke, Parkinson's disease, spinal cord injury, and multiple sclerosis.

CONFLICT OF INTERESTS

The authors declare no conflict of interests.

AUTHOR CONTRIBUTIONS

Ryan J. Downey built the device with consultation from Colleen A. Hanlon and Chris M. Gregory. Colleen A. Hanlon and Chris M. Gregory obtained the funding to support the project. Logan T. Dowdle and Julia P. Imperatore led the neuroimaging analysis. Jade D. Doolittle, Daniel H. Lench, and John McLeod ran the experimental sessions, compiled the data, and ran the data analyses. Jade D. Doolittle wrote the first draft of the manuscript which was edited and approved by all authors. All authors contributed to the writing and provided final approval.

DATA AVAILABILITY STATEMENT

The materials and instructions to construct the bipedal device are available in the supplemental section of this manuscript. The datasets used and/or analyzed during the current study are available upon reasonable request.

ETHICS STATEMENT

This study was approved by the Institutional Review Board of the Medical University of South Carolina and each participant gave written informed consent prior to participation in the study.

ORCID

Jade D. Doolittle https://orcid.org/0000-0002-1326-2507
Colleen A. Hanlon https://orcid.org/0000-0002-3151-0279

REFERENCES

Barut, C., Ozer, C. M., Sevİnc, O., Gumus, M., & Yunten, Z. (2007). Relationships between hand and foot preferences. *International Journal of Neuroscience*, *117*(2), 177–185. https://doi.org/10.1080/00207450600582033

Belforte, G., & Eula, G. (2012). Design of an active–passive device for human ankle movement during functional magnetic resonance imaging analysis. *Proceedings of the Institution of Mechanical Engineers, Part H: Journal of Engineering in Medicine*, *226*(1), 21–32. https://doi.org/10.1177/0954411911426946

Chen, G., Taylor, P. A., Haller, S. P., Kircanski, K., Stoddard, J., Pine, D. S., ... Cox, R. W. (2018). Intraclass correlation: Improved modeling approaches and applications for neuroimaging. *Human Brain Mapping*, *39*(3), 1187–1206. https://doi.org/10.1002/hbm.23909

Ciccarelli, O., Toosy, A. T., Marsden, J. F., Wheeler-Kingshott, C. M., Sahyoun, C., Matthews, P. M., ... Thompson, A. J. (2005). Identifying brain regions for integrative sensorimotor processing with ankle movements. *Experimental Brain Research*, *166*(1), 31–42. https://doi.org/10.1007/s00221-005-2335-5

Cicchetti, D. V. (1994). Guidelines, criteria, and rules of thumb for evaluating normed and standardized assessment instruments in psychology. *Psychological Assessment*, *6*(4), 284–290. https://doi.org/10.1037/1040-3590.6.4.284

da Cunha, I. T., Jr., Lim, P. A., Qureshy, H., Henson, H., Monga, T., & Protas, E. J. (2002). Gait outcomes after acute stroke rehabilitation with supported treadmill ambulation training: A randomized controlled pilot study. *Archives of Physical Medicine and Rehabilitation*, *83*(9), 1258–1265. https://doi.org/10.1053/apmr.2002.34267

de Lima-Pardini, A. C., de Azevedo Neto, R. M., Coelho, D. B., Boffino, C. C., Shergill, S. S., de Oliveira Souza, C., ... Amaro, E., Jr. (2017). An fMRI-compatible force measurement system for the evaluation of the neural correlates of step initiation. *Scientific Reports*, *7*, 43088. https://doi.org/10.1038/srep43088

Dobkin, B. H., & Dorsch, A. (2013). New evidence for therapies in stroke rehabilitation. *Current Atherosclerosis Reports*, *15*(6), 331. https://doi.org/10.1007/s11883-013-0331-y

Fontes, E. B., Okano, A. H., de Guio, F., Schabort, E. J., Min, L. L., Basset, F. A., ... Noakes, T. D. (2015). Brain activity and perceived exertion during cycling exercise: An fMRI study. *British Journal of Sports Medicine*, *49*(8), 556–560. https://doi.org/10.1136/bjsports-2012-091924

Grooms, D. R., Diekfuss, J. A., Ellis, J. D., Yuan, W., Dudley, J., Foss, K. D. B., ... Myer, G. D. (2019). A novel approach to evaluate brain activation for lower extremity motor control. *Journal of Neuroimaging*, *29*(5), 580–588. https://doi.org/10.1111/jon.12645

Hollnagel, C., Brügger, M., Vallery, H., Wolf, P., Dietz, V., Kollias, S., & Riener, R. (2011). Brain activity during stepping: A novel MRI-compatible device. *Journal of Neuroscience Methods*, *201*(1), 124–130. https://doi.org/10.1016/j.jneumeth.2011.07.022

Ikeda, T., Matsushita, A., Saotome, K., Hasegawa, Y., Matsumura, A., Sankai, Y., & Fukuda, T. (2015). *MRI compatibility of lower-extremity motion simulator: LoMS*. Paper presented at the 2015 IEEE International Conference on Robotics and Automation (ICRA).

Jaeger, L., Marchal-Crespo, L., Wolf, P., Riener, R., Michels, L., & Kollias, S. (2014). Brain activation associated with active and passive lower limb stepping. *Frontiers in Human Neuroscience*, *8*, 828. https://doi.org/10.3389/fnhum.2014.00828

Karim, H. T., Sparto, P. J., Aizenstein, H. J., Furman, J. M., Huppert, T. J., Erickson, K. I., & Loughlin, P. J. (2014). Functional MR imaging of a simulated balance task. *Brain Research*, *1555*, 20–27. https://doi.org/10.1016/j.brainres.2014.01.033

Kluding, P. M., Dunning, K., O'Dell, M. W., Wu, S. S., Ginosian, J., Feld, J., & McBride, K. (2013). Foot drop stimulation versus ankle foot orthosis after stroke: 30-week outcomes. *Stroke*, *44*(6), 1660–1669. https://doi.org/10.1161/strokeaha.111.000334

Labriffe, M., Annweiler, C., Amirova, L. E., Gauquelin-Koch, G., ter Minassian, A., Leiber, L. M., ... Dinomais, M. (2017). Brain activity during mental imagery of gait versus gait-like plantar stimulation: A novel combined functional MRI paradigm to better understand cerebral gait control. *Frontiers in Human Neuroscience*, *11*, 106. https://doi.org/10.3389/fnhum.2017.00106

Latham, N. K., Jette, D. U., Slavin, M., Richards, L. G., Procino, A., Smout, R. J., & Horn, S. D. (2005). Physical therapy during stroke rehabilitation for people with different walking abilities. *Archives of Physical Medicine and Rehabilitation*, *86*(12), 41–50. https://doi.org/10.1016/j.apmr.2005.08.128

Martinez, M., Villagra, F., Loayza, F., Vidorreta, M., Arrondo, G., Luis, E., ... Pastor, M. A. (2014). MRI-compatible device for examining brain activation related to stepping. *IEEE Transactions on Medical Imaging*, *33*(5), 1044–1053. https://doi.org/10.1109/tmi.2014.2301493

Mehta, J. P., Verber, M. D., Wieser, J. A., Schmit, B. D., & Schindler-Ivens, S. M. (2009). A novel technique for examining human brain activity associated with pedaling using fMRI. *Journal of Neuroscience Methods*, *179*(2), 230–239. https://doi.org/10.1016/j.jneumeth.2009.01.029

Milot, M. H., & Cramer, S. C. (2008). Biomarkers of recovery after stroke. *Current Opinion in Neurology*, *21*(6), 654–659. https://doi.org/10.1097/WCO.0b013e3283186f96

Newton, J. M., Dong, Y., Hidler, J., Plummer-D'Amato, P., Marehbian, J., Albistegui-Dubois, R. M., ... Dobkin, B. H. (2008). Reliable assessment of lower limb motor representations with fMRI: Use of a novel MR compatible device for real-time monitoring of ankle, knee and hip

torques. *NeuroImage*, *43*(1), 136–146. https://doi.org/10.1016/j.neuroimage.2008.07.001

Noble, J. W., Eng, J. J., & Boyd, L. A. (2014). Bilateral motor tasks involve more brain regions and higher neural activation than unilateral tasks: An fMRI study. *Experimental Brain Research*, *232*(9), 2785–2795. https://doi.org/10.1007/s00221-014-3963-4

Olszowy, W., Aston, J., Rua, C., & Williams, G. B. (2019). Accurate autocorrelation modeling substantially improves fMRI reliability. *Nature Communications*, *10*(1), 1220.

Papegaaij, S., Hortobagyi, T., Godde, B., Kaan, W. A., Erhard, P., & Voelcker-Rehage, C. (2017). Neural correlates of motor-cognitive dual-tasking in young and old adults. *PLoS One*, *12*(12), e0189025. https://doi.org/10.1371/journal.pone.0189025

Promjunyakul, N.-o., Schmit, B. D., & Schindler-Ivens, S. M. (2015). A novel fMRI paradigm suggests that pedaling-related brain activation is altered after stroke. *Frontiers in Human Neuroscience*, *9*, 324. https://doi.org/10.3389/fnhum.2015.00324

Sahyoun, C., Floyer-Lea, A., Johansen-Berg, H., & Matthews, P. M. (2004). Towards an understanding of gait control: Brain activation during the anticipation, preparation and execution of foot movements. *NeuroImage*, *21*(2), 568–575. https://doi.org/10.1016/j.neuroimage.2003.09.065

Trinastic, J. P., Kautz, S. A., McGregor, K., Gregory, C., Bowden, M., Benjamin, M. B., … Crosson, B. (2010). An fMRI study of the differences in brain activity during active ankle dorsiflexion and plantarflexion. *Brain Imaging and Behavior*, *4*(2), 121–131. https://doi.org/10.1007/s11682-010-9091-2

Wenning, G. K., Kiechl, S., Seppi, K., Muller, J., Hogl, B., Saletu, M., … Poewe, W. (2005). Prevalence of movement disorders in men and women aged 50-89 years (Bruneck study cohort): A population-based study. *Lancet Neurology*, *4*(12), 815–820. https://doi.org/10.1016/s1474-4422(05)70226-x

Williams, G., Schache, A., & Morris, M. (2012). Mobility after traumatic brain injury: Relationships with ankle joint power generation and motor skill level. *The Journal of Head Trauma Rehabilitation*, *28*(5), 371–378. https://doi.org/10.1097/HTR.0b013e31824a1d40

Xiao, X., Huang, D., & O'Young, B. (2012). Gait improvement after treadmill training in ischemic stroke survivors: A critical review of functional MRI studies. *Neural Regeneration Research*, *7*(31), 2457–2464. https://doi.org/10.3969/j.issn.1673-5374.2012.31.007

SUPPORTING INFORMATION

Additional supporting information may be found online in the Supporting Information section at the end of this article.